 doi:10.20944/preprints201705.0072.v1

Article

One-Step Synthesis and Sintering of Skutterudite $CoSb_3$: Smart Houses Materials?

Theodoros Giannakis[1,2,3,4], Alexandra Ioannidou[1,3,*],Dimitrios Niarchos[1,3], Konstantinos Karyofyllis[1], Meletis Saltas[4], Sofoklis S. Makridis[4,*]

[1] Institute of Nanoscience and Nanotechnology, NCSR Demokritos, Athens, Greece
[2] Department of Physics, National and Kapodistrian University of Athens, Greece
[3] AMEN Technologies, Athens, Greece
[4] Department of Environmental and Natural Resources Management, University of Patras, Greece
*a.ioannidou@amen-technologies.com; aioannidou@ims.demokritos.gr

Abstract: Thermoelectric materials may be used in devices as thermoelectric "air conditioner" in a smart house for improved energy efficiency. Energy harvesting uses ambient energy to generate electricity. It provides potentially low-cost, maintenance-free, long-life equipment by reducing the need for batteries or power chords. Energy harvesting (EH) is also known as power harvesting or energy scavenging. EH is considered to give benefits related to environmental friendliness, safety, security, convenience and affordability. EH can be used for brand enhancing. Technically, it can be used to make new things possible depending on visionary engineering. The variety of thermoelectric (TE) materials that can be used in energy harvesting is quite large, and the optimal material for a given application depends mainly on the temperature range in which the material is to be used. In this work we study the development and characterization of thermoelectric materials which were prepared by two different method, which were: a) ball-milling followed by sintering and b) ball-milling, microwave synthesis, high energy planetary ball milling, and sintering. Finally, we study the thermoelectric properties, calculate the band gaps and the ZT for the thermoelectric materials.

Keywords: Thermoelectric Materials; Energy Harvesting; $CoSb_3$; ZT

1. Introduction

World energy crisis has triggered more attention to energy saving and energy conversion systems along with economic efficiency. The global population is anticipated to have grown to 10 billion before the end of 21st century. The economic growth, increase in energy production, and global environmental protection represent a trilemma [1]. From the first law of thermodynamics, energy can neither be created nor destroyed. However we still need to be conservative in usage because of the efficiency, we cannot make full use of the energy. Large amount of energy is wasted. So how can we minimize energy waste and how can we reuse the wasted energy becomes critical in energy saving.

The field of Thermoelectricity (TE) advanced rapidly in the 1950s when the basic science of TE materials became well established. TE materials are important for specific applications e.g. satellites and space missions, equipment, and medical applications, where reliability, and predictability are very important. Thermoelectricity, which involves the conversion of heat into electricity and via versa, can play an important role in minimizing our dependency on fossil fuels [2]. Good TE materials must have a large dimensionless figure of merit which defined as $ZT = \frac{S^2\sigma}{\kappa}T$ [I], where S is the Seebeck coefficient, σ is the electrical conductivity, k is the thermal conductivity ($k = k_e + k_l$, where k_e is the electronic contribution and k_l is the lattice contribution), and T is the absolute temperature. The ZT value of a TE material can be improved by either increasing the electrical power factor $S^2\sigma$, decreasing the electrical conductivity k [3], or a combination of both.

 doi:10.20944/preprints201705.0072.v1

Skutterudite compounds have attracted much attention in the last decade as promising TE materials [4]. Materials with skutterudite crystal structure possess attractive transport properties and have a good potential for achieving ZT values substantially larger than innovative thermoelectric materials. The crystal structure is cubic with 32 atoms per unit cell (space group Im3) and contains two voids per unit cell. The void can be filled by several guest atoms. The filler atoms in the voids can play two roles. First, the filler atoms donate electrons into $CoSb_3$ framework, making the material n type. Second, the filler atoms in the voids are loosely bound with the neighboring atoms and have Einstein-like vibration, which act to scatter phonons and significantly reduce the lattice thermal conductivity [5].

$CoSb_3$ has been identified as a candidate for good thermoelectric materials because it has a large Seebeck coefficient and good electrical conductivity [6]. The thermal conductivity of $CoSb_3$ however is still high for being an efficient thermoelectric material. To lower the thermal conductivity and further to increase ZT value, great effort has been made in recent years. Filling the Sb-icosahedron voids by rare earth or other metallic atoms was usually used [7], which can optimize the electrical transport properties and significantly depresses the lattice thermal conductivity due to the rattling of these atoms. In addition, doping with Fe, Ni, Te and Pd atoms can also reduce the thermal conductivity due to the phonons scattering by the introduced point defects [8]. There have been many reports on improvements on thermoelectric properties of skutterudites by elemental substitution. A peak of approximately 0.9 at 530 °C was reported for $CoSb_{11.4}Te_{0.6}$ made by a solid-state reaction method followed by a spark-plasma sintering [9] and a peak ZT of ~1 at 530 °C in $CoSb_{2.625}Ge_{0.125}Te_{0.25}$ by melting-quenching-annealing method followed by spark-plasma sintering [10].

Thermoelectric materials may be used in devices as thermoelectric "air conditioner" in a smart house for improved energy efficiency. Energy harvesting uses ambient energy to generate electricity. It provides potentially low-cost, maintenance-free, long-life equipment by reducing the need for batteries or power chords. Energy harvesting (EH) is also known as power harvesting or energy scavenging. EH is considered to give benefits related to environmental friendliness, safety, security, convenience and affordability. EH can be used for brand enhancing. Technically, it can be used to make new things possible depending on visionary engineering. The variety of thermoelectric (TE) materials that can be used in energy harvesting is quite large, and the optimal material for a given application depends mainly on the temperature range in which the material is to be used. Although thermoelectric materials exhibit thermoelectric behaviour at all temperatures, their figure of merit (ZT) is quite strongly influenced by temperature, and the ZT value typically peaks in a certain temperature range. When evaluating the feasibility of thermoelectric materials for different applications, the material performance in the required temperature range, in addition to other factors like cost and availability, should therefore be taken into account.

Nanostructuring has led to significant improvement in the properties of thermoelectric materials. The main strategy has been to decrease the thermal conductivity via phonon scattering. Research is required to understand the interaction between thermal, electrical and entropy transport; controlling nanostructures that can be used in actual devices; and improvements in materials for soldering, ceramics, packaging, etc.

The main focus of the research is still on tellurides due to their outstanding properties. Some of the most interesting alternatives to make cheap and less toxic TE materials include Mg_2Si, $CoSb_3$, ZnSb, ZnO and other oxides. All these materials have been known about for a long time. More explorative work is required to find completely new materials.

In this work we study the development and characterization of thermoelectric materials which were prepared by two different method, which were: a) ball-milling followed by sintering and b) ball-milling, microwave synthesis, high energy planetary ball milling, and sintering. Finally, we study the thermoelectric properties, calculate the band gaps and the ZT for the thermoelectric materials.

2. Experimental Procedures

The samples were prepared with Co (99.8 purity, Sigma-Aldrich) and Sb (99.5 purity, Sigma-Aldrich) powders as sources, which were weighed according to the stoichiometric ratio of $CoSb_3$.

 doi:10.20944/preprints201705.0072.v1

2.1. First Method (Ball Milling)

The powders were uniformly mixed with stainless balls in a planetary mill (Fritsch PQ-N04) for 2 h, the mixtures were enveloped by graphite foil and were loaded into a cylindrical graphite die with diameter of 15 mm, where then sintered into bulk samples by a Compact RF Sintering System (AMEN Technologies). Table 1 shows analytically the temperature, the force, and the total time of the sintering.

Table 1. Sintering temperature, Sintering force, and Sintering time.

Sample	Sintering Temperature (°C)	Sintering Force (KN)	Sintering Time (min)
BM1/MW1	550	9	6
BM2/MW2	550	9	8
BM3/MW3	580	9	5
BM4/MW4	580	9	8
BM5/MW5	600	9	6

2.2. Second Method (Microwaves)

Such as the first method, the powders were mixed with stainless balls in a planetary miller for 2 h, the mixtures were cold-pressed in pellets and sealed in evacuated quartz tubes. The sealed quartz tubes were placed into a crucible filled with Copper oxide powder (98% purity, Sigma-Aldrich) which act as microwave susceptor material. The whole set up was placed into a commercial microwave reactor with rotate plate (Panasonic NE-1856). The reactions were allowed to run at 900 W for 4 min and at 450 W for 10 min. Every sample allowed to cool before it was removed from the microwave. The samples were crushed using a percussion mortar and ground into small pieces. In order to obtain a fine powder, the small pieces were ball milled for 15 min (Spex-8000 M Mixer/Mill). The powders were enveloped by graphite foil and were loaded into a cylindrical graphite die with diameter of 15 mm, where then sintered into bulk samples by a Compact RF Sintering System (AMEN Technologies). Table 1 shows the temperature, the force, and the total time of the sintering.

For both methods the crystallographic phase of the samples was characterized by X-ray diffraction (XRD, Seifert 3003 TT) with Cu-K_α radiation (λ=1.54059 Å), and the microstructure was analyzed by scanning electron microscopy (SEM, Phenom ProX). The thermal conductivity of the samples (15mm diameter and 3mm thickness) is characterized using a four-probe, steady-state electrothermal measurement technique based on the ASTM D5470-06 standard, in the range (300-700) K. Every sample was cut into bar (2 x 2 x 12) mm^3 to measure the electrical conductivity and the Seebeck coefficient, which been achieved using a commercial equipment based on the ZEM-3 standard in the range 300 K to 700 K.

3. Results and Discussion

Figure 1 shows the XRD patterns of $CoSb_3$ samples which prepared by the two different methods in a range of $2\theta = 10^o$-90^o. It can be seen that all the samples are single-phase materials with a minute amount of Sb and $CoSb_2$.

Preprints (www.preprints.org) | NOT PEER-REVIEWED | Posted: 8 May 2017 doi:10.20944/preprints201705.0072.v1

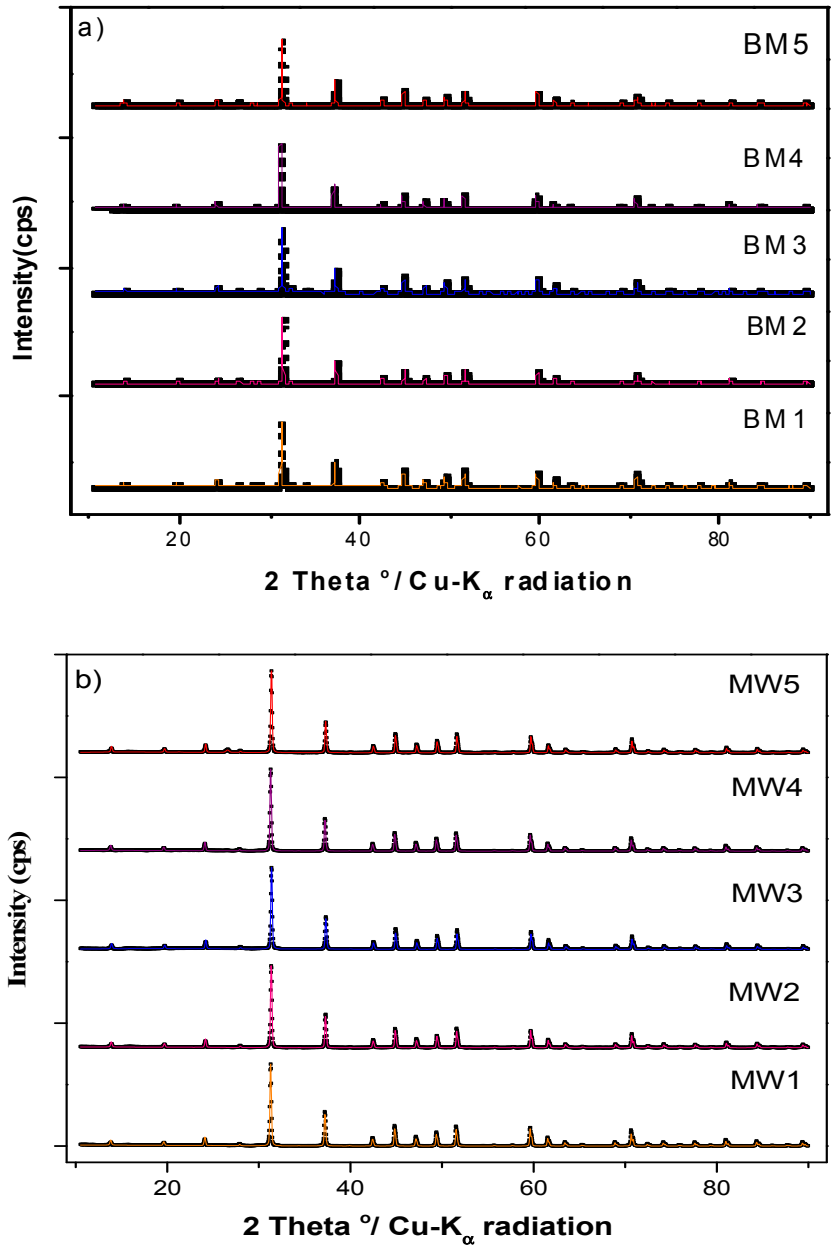

Figure 1. XRD patterns of $CoSb_3$ samples, (**a**) first method: ball milled; (**b**) second method: Microwaves.

Moreover the Figure 2 shows the XRD pattern of BM2 sample which displays the lowest R_{Bragg} residual factor for the main phase. The presence of SiO_2 is due to a fragment of quartz which created during of its smashing in order to release the sample BM2.

Preprints (www.preprints.org) | NOT PEER-REVIEWED | Posted: 8 May 2017 doi:10.20944/preprints201705.0072.v1

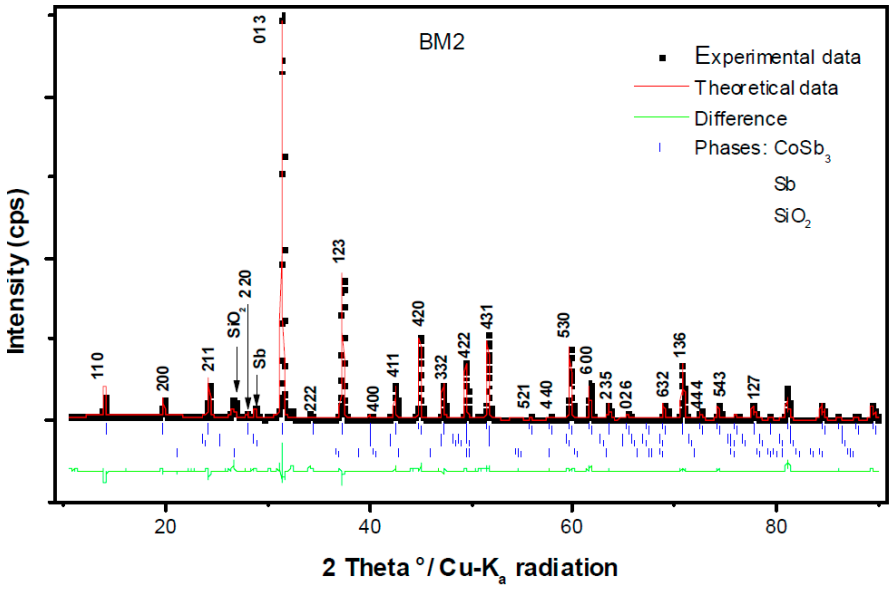

Figure 2. XRD pattern of BM2 sample.

Table 2 summarizes the lattice parameters, the weight percentage of the phases and the residual factors R_{Bragg}, R_{wp}, R_p, and R_{exp} which obtained from Rietveld refinements of the synchrotron XRD data for the sample BM2. The refined lattice constants of $CoSb_3$ match those reported in the literature [9] and only very small deviations are observed for the individual samples.

Table 2. Lattice parameters, weight percentage of phases R_{wp}, R_p, and R_{exp} of sample BM2.

	$CoSb_3$	**Sb**	**SiO_2**
Lattice parameters (Å)	a=b=c=9.035	a=b=4.305 c=11.314	a=b=4.891 c=5.529
Weight percentage of phases	94.80 %	3.30 %	1.90 %
R_p		10.71	
R_{wp}		15.94	
R_{exp}		5.22	

SEM images of $CoSb_3$ sample BM2 shown in Figure 3 .These images reveal that the sample have a uniform microstructure and surface morphology. However in some cases, as we can observe in the spot 1 of the Figure 2b, the scanning electron microscope shows that the Sb phase distributes in the form of clusters with micron dimension. The EDAX analysis of the samples which is shown in Table 3 reveals that the average composition is very close to the nominal ratio Sb/Co = 3:1.

 doi:10.20944/preprints201705.0072.v1

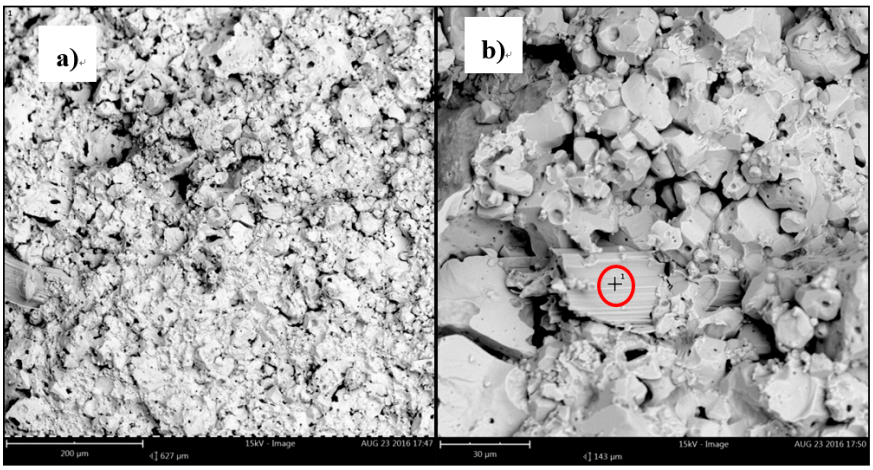

Figure 3. SEM images of the cross-section of sample BM2.

Table 3. EDAX analysis of $CoSb_3$ samples.

Sample	Atomic percentage of Sb (%)	Atomic percentage of Co (%)
BM1	79.2	20.8
BM2	81.8	18.2
BM3	79.9	20.1
BM4	78.5	21.5
BM5	78.0	22.0
MW1	78.6	21.4
MW2	78.5	21.5
MW3	78.0	22.0
MW4	76.4	23.6
MW5	78.3	21.7

The electrical conductivity of the samples as a function of temperature is plotted in Figure 4. From the plot we observe that, the electrical conductivity of each sample increases with temperature over the measured range, indicating semiconductor behavior. In addition, we can observe that the second method gives us almost the same results for the five samples, something that we can't notice in the first method. This phenomenon may be largely due to the presence of Sb which we have as secondary phase in the first method, because it can lead to an electrical conductivity increase [11].

Preprints (www.preprints.org) | NOT PEER-REVIEWED | Posted: 8 May 2017 doi:10.20944/preprints201705.0072.v1

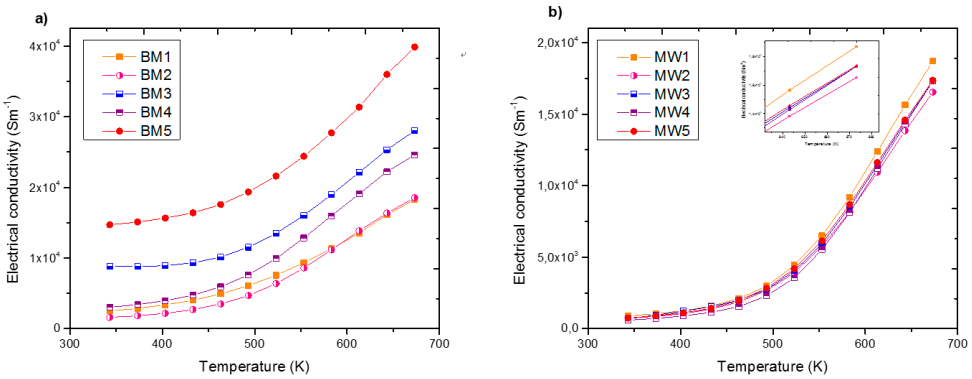

Figure 4. Temperature dependence of electrical conductivity of samples, (**a**) first method; (**b**) second method.

In Figure 5, the Seebeck coefficient is plotted as a function of temperature from 300 K to 700 K. Initially almost all the samples (except from BM3) show n-type conduction with negative Seebeck coefficients. For the first method we can't have useful conclusions for the switching sign of Seebeck coefficient because of the existence of secondary phases in different percentages. However, in the second method the Seebeck coefficient changes to positive approximately at 540 K. The reason is that the hole mobility is much larger than the electron mobility in the temperature range higher than 540 K [12], at which intrinsic excitation commences. It has been reported that the intrinsic $CoSb_3$ shows the p-type conductivity [13, 14]. In this study, the low purity of Co (99.8%) may be the reason for the appearance of n-type conductivity initially [15]. From the temperature-dependent Seebeck coefficient measurement, the band gap E_g of various samples can be roughly estimated using the equation $E_g = 2eS_{max}T_{max}$ (II), where e is the elementary charge, S_{max} is the peak Seebeck coefficient, and T_{max} is the temperature corresponding to the maximum Sebeck coefficient [16]. Based on this equation the energy gaps of the samples were estimated to be in the range of 0.09-0.29 eV (table 4), which is consistent with the values reported in literature [17].

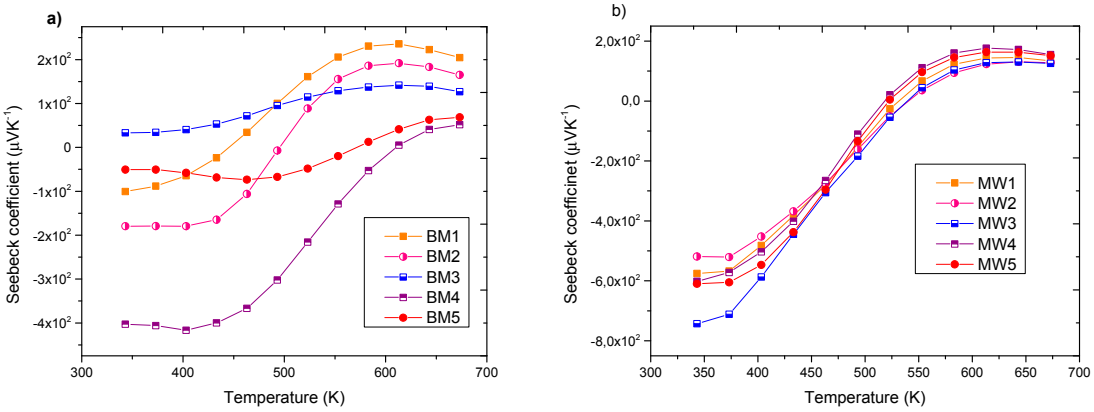

Figure 5. Temperature dependence of Seebeck coefficient of samples, (a) first method, (b) second method.

The temperature dependence of thermal conductivity for the two methods is shown in Figure 6. It is clear that the thermal conductivity of the most samples increases with the increasing temperature. The increase of k in some samples is due to the increase of the grain size. Significant role play the grain boundaries which could scatter phonons and decreases the thermal conductivity. At high temperatures, acoustic phonon scattering is mostly responsible for the decrease in thermal conductivity with a T^{-1} dependence [18].

Preprints (www.preprints.org) | NOT PEER-REVIEWED | Posted: 8 May 2017 doi:10.20944/preprints201705.0072.v1

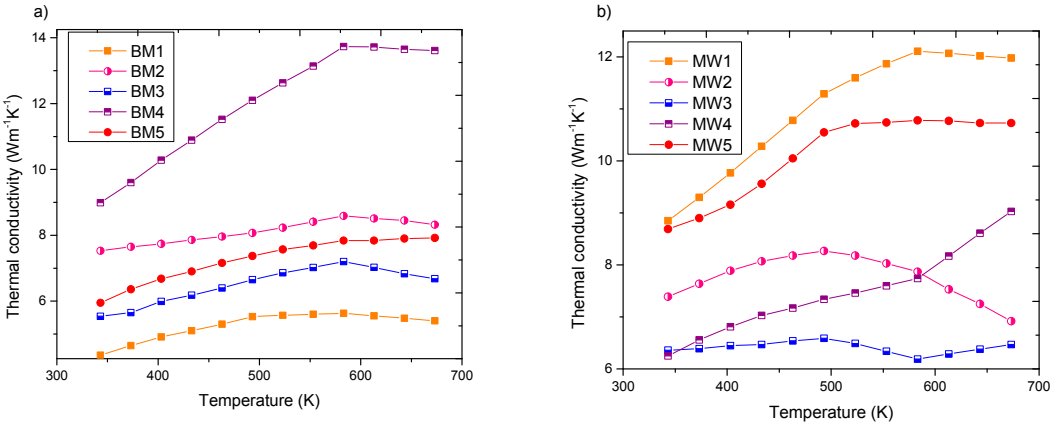

Figure 6. Temperature dependence of thermal conductivity of samples, (a) first method, (b) second method.

The calculated dimensionless figure of merit ZT values are shown in Figure 7. As we can observe all the ZT are in a range of 0.02-0.10. The maximum value of ZT is 0.10 for the BM1 sample at 673 K. The combination of low thermal conductivity and the high Seebeck coefficient are the reasons which the sample BM1 has highest figure of merit. Moreover it's obviously that in the second method we have a minimum for all the samples approximately at 540 K. The reason is that at 540 K the Seebeck coefficient changes sign from negative to positive.

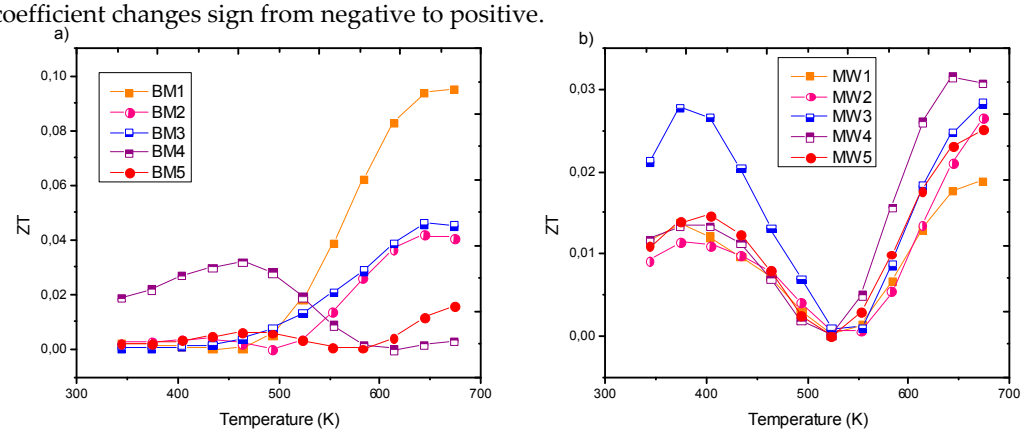

Figure 7. Temperature dependence of ZT of samples, (a) first method, (b) second method

 doi:10.20944/preprints201705.0072.v1

Table 4. Band gaps of samples

Sample	Tmax (K)	Smax (μVK^{-1})	Eg (eV)
BM1	613.15	235.66	0.29
BM2	613.15	191.87	0.24
BM3	613.15	141.62	0.17
BM4	673.15	51.55	0.07
BM5	673.15	68.71	0.09
MW1	643.15	145.35	0.19
MW2	643.15	130.75	0.17
MW3	643.15	130.52	0.17
MW4	613.15	176.35	0.22
MW5	613.15	163.42	0.20

Recommendations given include further material science research on materials structure, electrical properties and performance, as well as processing and manufacturing to overcome obstacles related to price and production up-scaling. The work requires multi-disciplinary activity and co-operation. The utilization of advanced modelling supports the required multi-disciplinary actions. All above techniques may develop new materials for energy harvesting and the uses in smart houses and key technologies in smart cities.

Conclusions

In this work, skutterudite $CoSb_3$ was prepared by two different methods. From the results which we have from the XRD patterns and SEM we can conclude that the first method can give us a single step synthesis of $CoSb_3$ alloys. One step synthesis can reduce dramatically the time for the growth of the samples compared to conventional or microwave methods. XRD analysis has revealed that the samples of the second method with microwaves are of single phase contrary to the ball milled where Sb is present as micrograin. The small Sb percentage may be connected with the abnormal behavior of the temperature dependence of Seebeck coefficient values of the ball milled samples while no sign of connection of the XRD to the microstructure and the electrical parameters is visible. The single phase of the microwaved powders is responsible of the normal temperature dependence of Seebeck coefficient for all sample. This is also reflected in the electrical, thermal conductivity, the Seebeck coefficient and the figure of merit ZT. The energy bands of the samples were estimated to be in the range of 0.09-0.29 eV, which is consistent with the values reported in literature. The highest value of figure of merit ZT obtained by BM1 sample which was growth by the first method and sintered for 6 min. under 9 KN force at 823 K.

References

1. Levy B., J. Electroceram., 1, 239 (1997)
2. M. S. Dresselhaus, G Chen, M. Y. Tang, R.Ynag, H. Lee, D. Wang, Z. F. Ren, J. P. Fleurial and P. Gogna, Adu. Mater. 19, 1043 (2007)
3. R. H. Tarkhanyan, A. Ioannidou, and D.G. Niarchos, The Minerals & Materials Society and ASM International (2014)
4. J. P. Fleurial, T Caillat and A. Borschevsky, Proceedings of the XVI International Conferece on the Thermoelectrics, Dresden, Germany (1997)
5. W. F. Leonrad and T. J. Martin Jr. ,Electronic Structure and Transport Properties of Crystals, (1979)
6. D. Mandrus, A. Migliori, T. W. Darling, M. F. Hundley, E. J. Peterson, J. D. Thompson, Phys. Rev. 50, 4926 (1995)
7. Y. Z. Pei, S. Q. Bai, X. Y. Zhao, W. Zhang, L. D. Chen, Solid State Sci.10, 1422 (2008)
8. M. Chitroub, F. Besse, H Scherre, J. Alloys Compd. 467, 31 (2009)

 doi:10.20944/preprints201705.0072.v1

9. B. Duan, P. Zhai, L. Liu, Q. J. Zhang, and X. F. Ruan, J. Mater. Sci. Mater. Electron. 23, 1817 (2012)
10. X. Su, L. Han, Q. H. Guo, X. F. Tang, Q. J. Zhang, and C. Uher, J. Electron. Mater. 40, 1286 (2011)
11. P.-F. Wen, P. Li, Q.-J. Zhang, Z.-W. Ruan, L.-S. Liu, and P.-C. Zhai, J. Electron. Mater. 42,1443 (2013)
12. W.-S. Liu, B.-P. Zhang, J.-F. Li, H.-L. Zhang, L.-D. and Zhao, J. Appl. Phys. 102, 103717 (2007)
13. I.-H. Kim, K.-H. Park, and S.-C. Ur, J. Alloys Compd. 442, 351 (2007)
14. O. Prytz, O.M. Lovvik, and J. Tafto, Phys. Rev. B. 74, 245109 (2006)
15. Y. Zhu, H. Shen, and H. Guan , J. Mater. Sci. Mater. Electron. 23, 2210 (2012)
16. G. J. Goldsmith, and J. W. Sharp, J. Electron. Mater. 28, 869 (1999)
17. D. Mandrus, A. Migliori , T. W. Darling, M. F. Hundley, E. J. Peterson, and J. D. Thomspon, Phys. Rev. B 52, 4926 (1995)
18. T. Caillat, A. Borshchevsky, and J. P. Fleurial, J. Appl. Phys. 80, 4442 (1996)